OWL wind loading characterization: a preliminary study

Marco Quattri[1], Franz Koch[1], Lothar Noethe[1], A. Correal Bonnet[2], S. Nölting[3].

[1] European Southern Observatory
Karl Schwarzschildstrasse, 2
D-85748 Garching, Germany

[2] CadFem GmbH
Geschäftsstelle Stuttgart
Hauptstrasse, 111
D-70771 Leinfelden-Echterdingen

[3]EXA GmbH
Nobelstrasse, 15
D-70569 Stuttgart, Germany

ABSTRACT

The 100-m OWL telescope being considered for open-air operation, wind is an essential disturbance affecting the tracking performance and figure of the primary and secondary mirrors. ESO has undertaken a study to build up a reliable and flexible computer model of the telescope and its environment. This model can, in a cost-effective way, be used to assess the wind loading under different conditions and configurations, before entering into more expensive wind tunnel testing. This paper presents the first preliminary results obtained with Computational Fluid Dynamic (CFD) methods about the wind action on the OWL 100-m telescope, in terms of pressure time histories and in the frequency domain. Preliminary conclusions on the effect of the wind loading on the design are also drafted.

Keywords: OWL, Large telescopes, wind.

1. INTRODUCTION

The characterization of the wind loading on structures is crucial for the assessment of the performance of telescopes, especially if the facility is planned to operate in open air as in the case of OWL.
During the design phase it is important to set a reliable procedure, which gives the capability to assess the performances of different designs and allows feedback for design iteration.
Wind action is in its nature stochastic and therefore the Power Spectral Density (PSD), either of the wind speed or of the aerodynamic pressure on the surfaces, is a convenient way to characterize dynamics loads.
In the design phase mainly four possible approaches to wind PSD determination are used in industrial environment:

1. **Use of the established wind PSD shapes proposed in literature**. ESO has made wide use of this approach in the VLT design phase. The von Karman spectrum has been found to adequately represent the wind energy content in the frequency domain on the typical observing site. The von Karman spectrum characterizes the energy content of wind in the frequency domain using three parameters:
   - The mean wind velocity, $\bar{U}$.
   - The integral scale of turbulence, which gives information on the average size of the turbulent eddies in the stream, and which is obtained from the autocorrelation function of the turbulent velocity [1]

$$R_u = \frac{\int_0^{T_0} u(t)u(t+\tau)dt\,\tau}{\int_0^{T_0} u^2(t)dt}$$

     where u(t) is the turbulent velocity and u(t+τ) is the turbulent velocity at the time (t+τ).
   - The turbulence intensity, which is defined as the ratio of the standard deviation of the wind speed divided by the mean speed

$$I = \frac{\sigma_u}{\overline{U}}.$$

Once these parameters are set the von Karman spectrum of the wind speed assumes the well-known form

$$S_U(f) = \left(I\overline{U}\right)^2 \frac{4L}{\overline{U}} \frac{1}{\left[1+70.78\left(f\frac{L}{\overline{U}}\right)^2\right]^{\frac{5}{6}}}$$

Where $\bar{U}$ is the mean speed, L is the integral scale of turbulence, I is the turbulence intensity and f is the frequency.

In order to take into account the interaction between structure and wind flow, which modifies the wind PSD at higher frequencies, Vickery [2] suggested in 1965 to correct the PSD using the following empirical formula for the aerodynamic admittance function

$$\chi_a(f) = \frac{1}{1+\left(2f\frac{\sqrt{A}}{\overline{U}}\right)^{\frac{4}{3}}}$$

Where A is the aerodynamic area characteristic of the structure being analyzed. In conclusion this approach requires guessing a number of flow and flow related structural parameters upon which the resulting wind PSD substantially depends. The process of guessing those parameters is delicate and is mainly based on experience, or on existing cases judged meaningful for the case studied. In the VLT case ESO performed wind tunnel tests on models to validate the assumptions taken at the time of the design process. Also the uncritical use of the aerodynamic admittance function, which greatly lowers the wind energy content at high frequencies for large structures, may lead to erroneous results, as will become clear in the following. Moreover the results given by the use of the established industrial approach outlined above loose validity if the interaction between wind and structure happens in a region of flow re-circulation or at high turbulence intensity (higher than 25-30%).

2. **Performance of wind tunnel tests**. It is arguably the most valuable approach to wind analysis. In the case of VLT it has been widely used to study wind action on the telescope tracking and to characterize the effect of the presence of a building around the telescope. It has been used also to study the turbulent pressure distribution and spatial correlation on mirror surfaces. The main difficulty of this approach when used at the early stage of a project, is that one has to prepare hardware models which need to be modified to study different configurations. The necessity to do testing in boundary layer wind tunnel limits the availability of the facilities. Matching turbulence intensity and integral scale of turbulence is also a difficulty, and matching the Reynolds number sometime limits the scale of the model that can be tested. Nevertheless wind tunnel testing is a stage that wind loading assessment should always undergo to. It is the most meaningful way to determine pressure distribution on surfaces, reaction forces, turbulent flow parameters, time and space correlations of the turbulent parameters. It is advisable to perform the wind tunnel test on a design that has been already evaluated by other means, such as Computational Fluid Dynamic (CFD).

3. **Computational Fluid Dynamic (CFD)**. A method to study fluid flow is provided by CFD. This approach requires powerful computing facilities and in the past could be used only for simple geometries and flows with limited turbulent content. Most of the computer programs solve the complete Navier-Stokes equations and very much care must be dedicated to the stability of the solution. Since the development of computer programs, that use the lattice Boltzmann method approach to deal with particle dynamics, accurate and stable solutions for turbulent flow are easier to obtain than in the past. CFD became then an effective mean to characterize both steady and transient flow parameters. It gives the possibility to calculate accurate and unconditionally stable velocity and pressure time histories in highly complicated geometries and high Reynolds numbers. Wind pressure on surfaces, global reactions, flow speed can be calculated in a number of points of interest which act exactly like instrumented points in a wind tunnel model.

4. **Full scale measurements**. This is of course the best way to characterize the wind flow loading on a structure. It may be possible for small structures. It may also represent a viable method if a structure comparable to the one being designed exists. The main difficulty is to extend the results to the actual case, for instance because of different input wind PSD due to differences in the horography of the site or of terrain roughness.

For OWL we plan to use the last three methods to characterize the dynamic of the wind loading on the telescope structure and on the mirror surfaces. As a first step CFD has been used to calculate the PSD of a 10 m/s speed wind hitting the telescope with an attack angle of 20° both in azimuth and altitude. The PSD's are used to calculate the response PSD's of the telescopes segmented primary and secondary mirror. This allows assessing the frequency content of the resulting displacements, on this basis the controllability of the surface of the mirrors can be assessed, and a control strategy determined.

2. CFD ANALYSIS

In view of its dynamic nature wind loading on a telescope must be characterized in the frequency domain. For this reason, and in order to have highly stable solutions, we chose to use PowerFLOW® [3] CFD computer program. PowerFLOW DWT™ has the capability to act as a numerical wind tunnel. In the last ten years this CFD program has been used worldwide to simulate flows in and around bodies, including buildings, and has earned a large benchmark database, proving to be a very accurate and robust tool. The structure/telescope to be studied is modeled and placed into the numerical wind tunnel. The complete volume is filled with voxels, which represent the elementary volumes in which the wind enters and interacts in accordance with the laws of conservation of mass, momentum and energy. The wind enters the numerical wind tunnel starting already with a velocity profile typical of the one developed in open terrain with low vegetation and asperities. It develops a turbulence in accordance with the specified boundary conditions, and develops further while interacting with any obstacles it encounters. In OWL specific case the model is shown in figure 1. The model is composed of about 16 millions voxels with dimensions ranging from 0.4m, in the region in which high turbulence is expected to develop, to about 20m in the region of expected undisturbed flow. The smallest dimension of the voxel defines together with the integration time step, which is equivalent to the sampling time of the pressure signal, the highest frequency of turbulence, which can be resolved in the calculation.

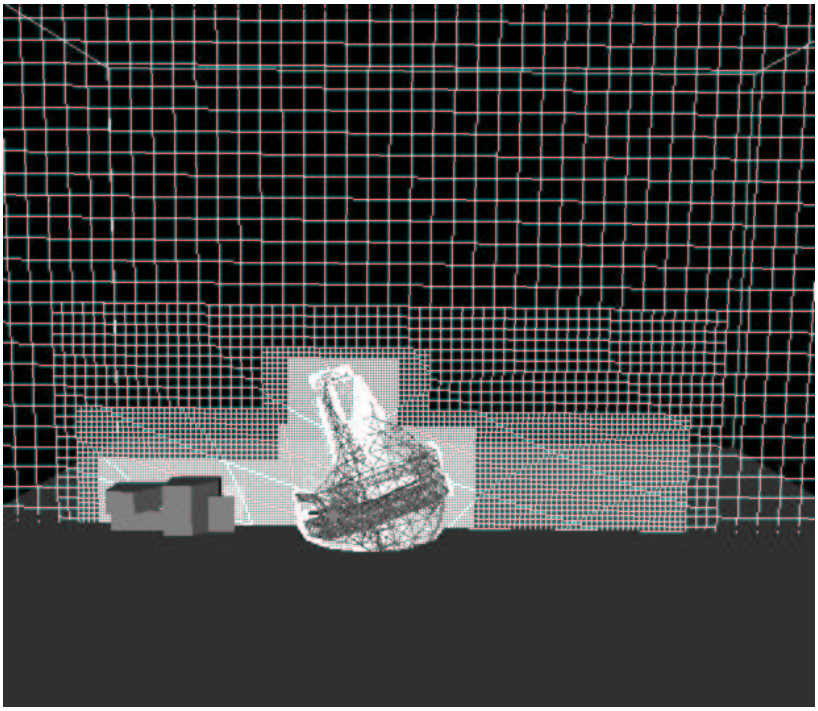

Figure 1: CFD model of OWL**.**

For the first load case the wind speed has been set at 10m/s, The entry profile is defined for open terrain with low roughness, and is of the type

$$\overline{U(z)} = \overline{U(z_{ref})}\left(\frac{z}{z_{ref}}\right)^{\alpha}$$

Where z is the vertical coordinate and α is set to 0.14 to consider the conditions described above [1]. The telescope azimuth and altitude axes are set at 20º, conditions which was found in the past, during the VLT study, as one of the worst in terms of wind loading onto the telescope structure.

Two analyses have been performed: with and without maintenance building. One of the main objectives of this study was to define whether any obstacle placed in front of the telescope would have caused the wind PSD to have larger

energy at higher frequency. This situation, which is widely substantiated by VLT studies and in literature, must be avoided, being the higher time frequency deformation much more difficult to correct than large deformation at low frequencies.
Five hundred control points have been uniformly placed on the optical surfaces and on the telescope structure (see Fig. 2). In these points the pressure time histories arecalculated and saved, allowing the PSD of the wind pressure to be determined.

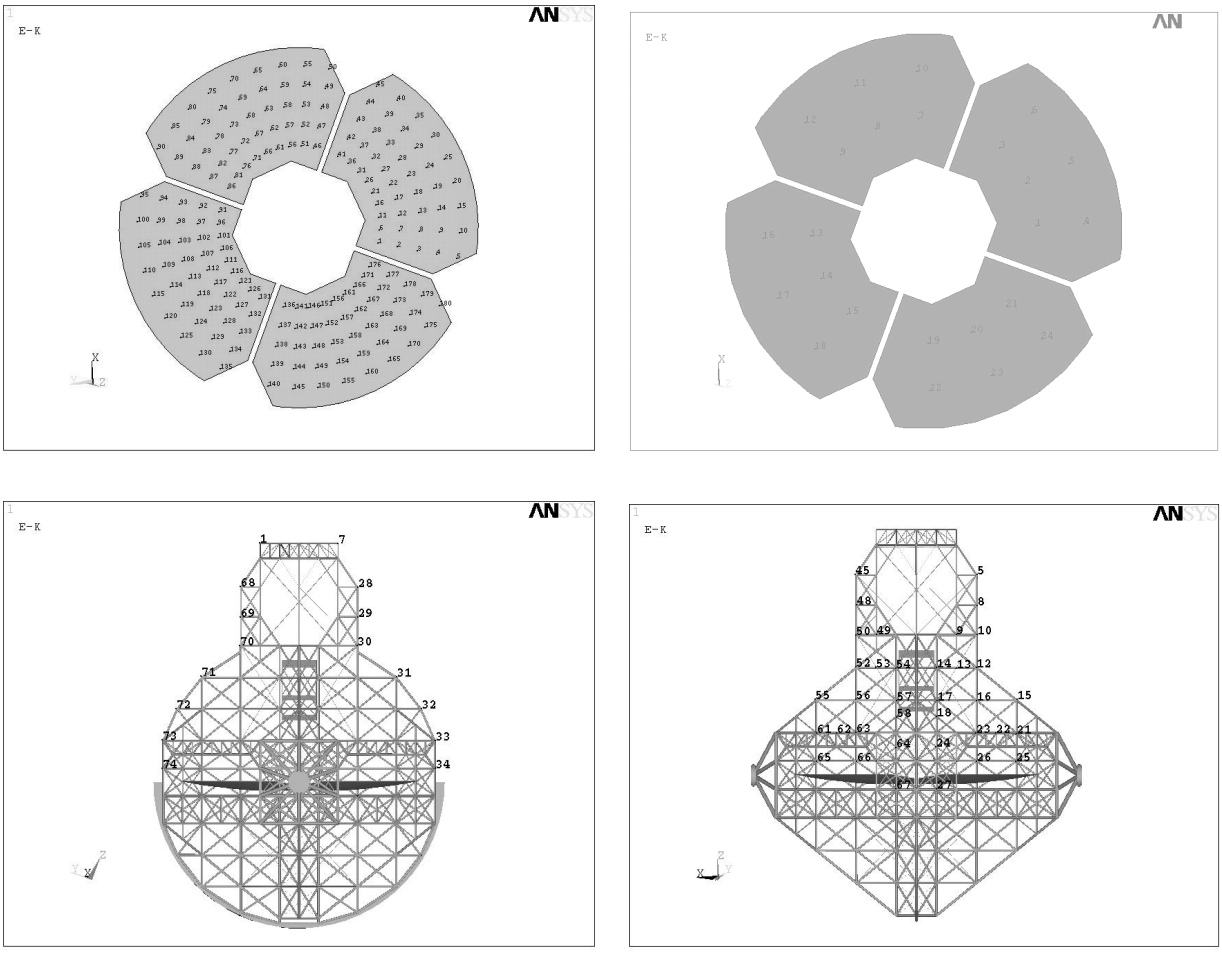

Figure 2: Some of the 500 control points in the model (M1, top left; M2, top right; telescope structure, bottom).

The pressure time history is calculated on a time scale, which assures the complete development of a stationary behavior in statistical terms. In other words the history has exhausted large oscillations or its trend to diverge.
In the case of OWL two different discretizations have been tested, with a difference in size of the voxels. This was done to test the overall validity of the results and to appreciate the differences in the development of a stochastic stationary pressure field. The results was that in the case with 18% smaller voxels the full development of the turbulent flow was reached in about 200s simulation instead of 500 s as for the larger voxels dimension.
In the case of finer meshing a single run takes a total of 1066 CPU hours (1 hour/processor to simulate 6s of time history). The capability of PowerFLOW to run in parallel on several processors allowed the complete analysis to be completed within about 35 hours on a 32-processor machine.
It is clear that the use of powerful computers is crucial for obtaining results in reasonable time frame (time about proportional to the number of processors).

3. CREATION OF INPUT PSD

The outcome results of a PowerFlow analysis are:

- Speed time histories in defined volumes other then the control points, in which only pressures can be saved for further processing. Velocity stream lines as shown in Fig. 3.
- Pressures all over the surfaces every 1s (see Fig.4).
- Time histories of the pressure fluctuation at the different control points, every single integration time step (0.01025s) (see Fig. 5).

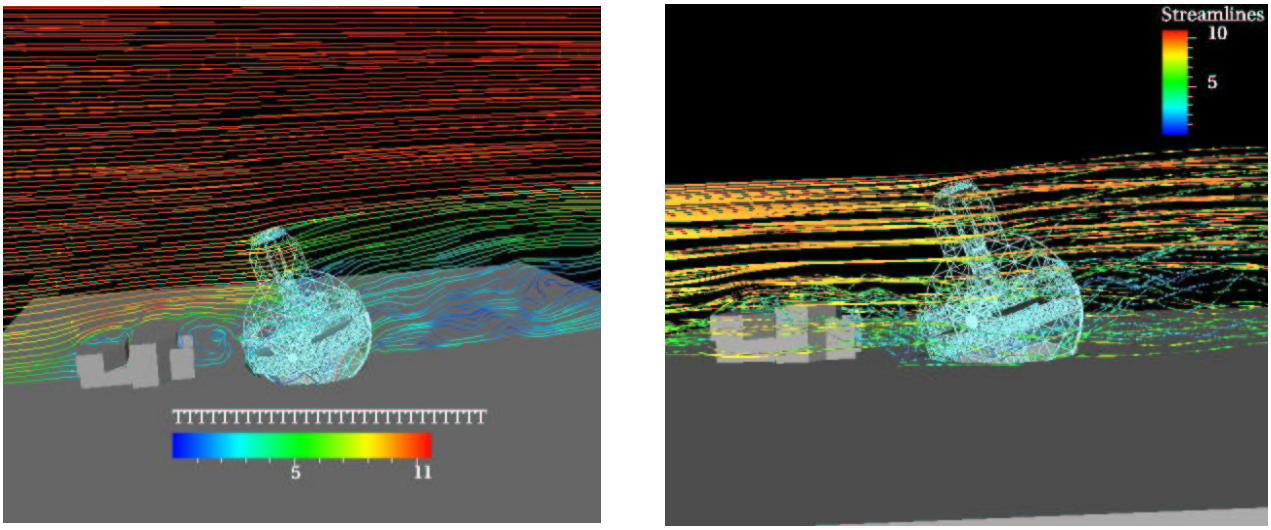

Figure 3: Velocity stream lines. Turbulent regions and re-circulation regions can be seen after the building and M1

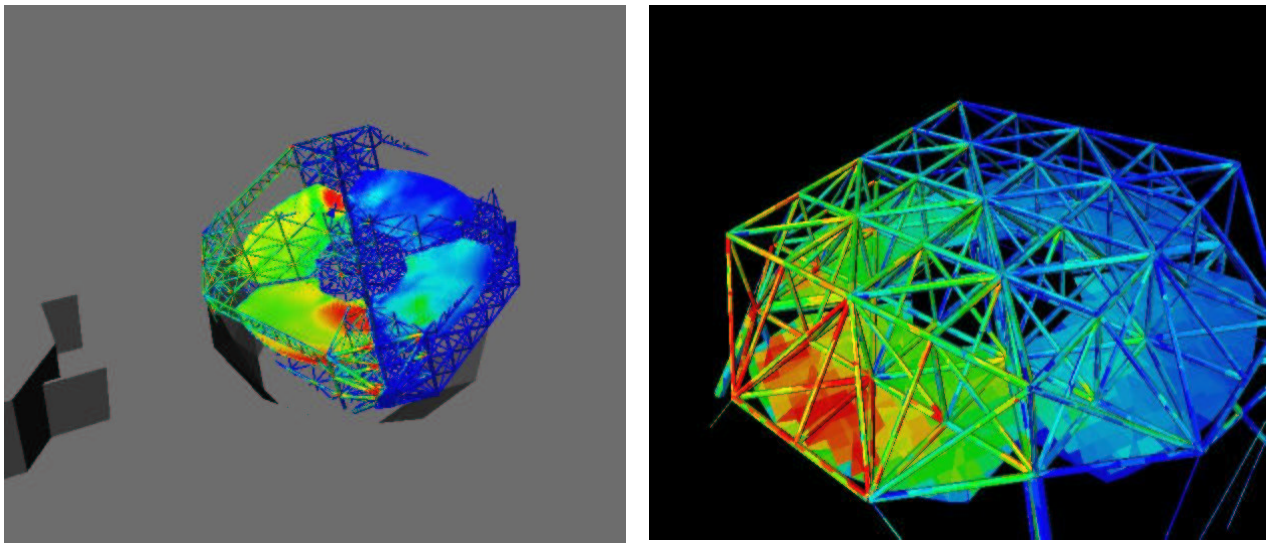

Figure 4: Pressure distributions on M1 (Left) and M2 (right)

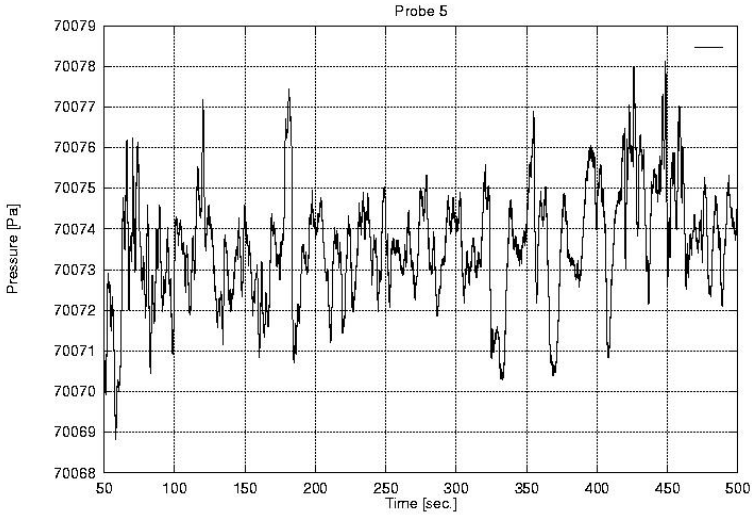

Figure 5: typical pressure time history.

Starting from the time histories and using Fourier Transform one calculates the PSD in the different control points, which will be then used to calculate deformations using random vibration theory.
In doing this one has to recall that a number of peaks deriving from the geometrical discretization and from the sampling time of the signal (pressure in this case) will be present in the calculated spectra. In the present case the Nyquist frequency is about 48.8 Hz, therefore a peak will show up at this frequency and its sub-harmonics in the PSD. Also special care is to be taken in the PSD derivation because of the numerical noise injected by the Fast Fourier Transform (FFT) algorithm at higher frequencies. This spreads the tail of the spectra, which leads to higher energy estimation in the case one uses an envelope to compute response PSDs.
A typical PSD is shown in Fig. 6 for the case with and without building.

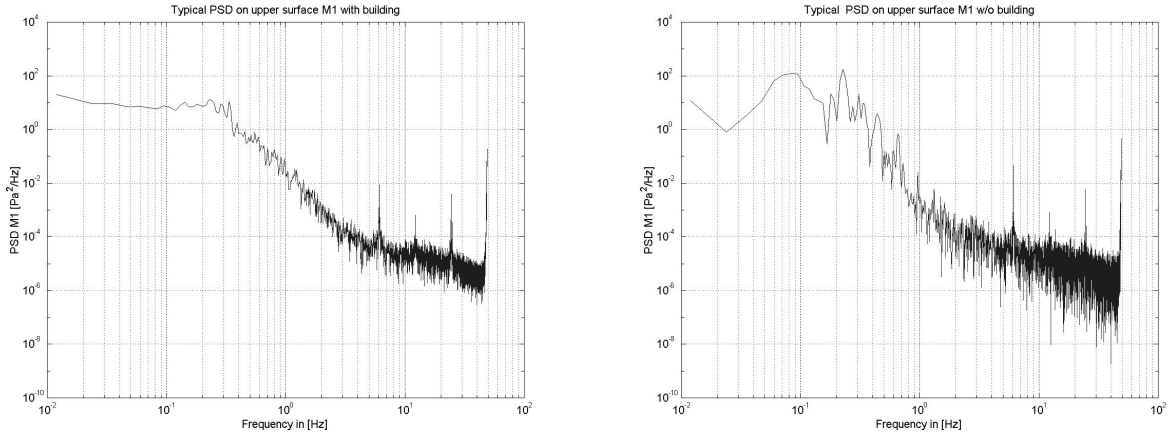

Figure 6: typical PSD with building (left), without building (right).

The spurious peaks are clearly seen, as well as the numeric noise at higher frequencies. The numeric noise is larger in the case without building because the averaging has been applied to a shorter time record, therefore it is equivalent to having a low averaging.
In order to perform the calculations of the mirrors deformations under wind pressure it was decided to apply the approach normally used in the cases where many spectra are available on the same structure, that is to make the best fit of the envelope of all of them. The resulting spectra for M1 with and without building are shown in Fig 7.

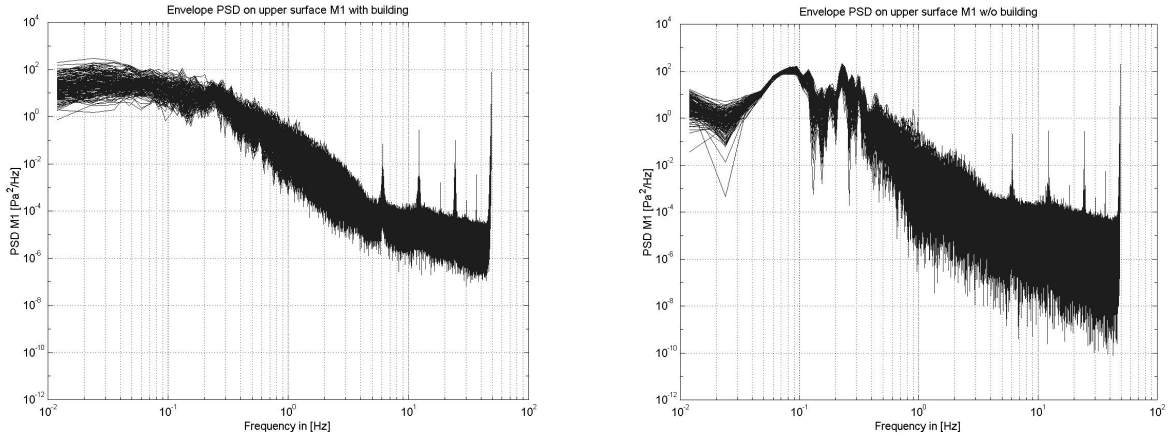

Figure 7: Envelope of all 180 PSDs on M1. With building (left), without building (right).

The decision to use the best fit of the spectra came from an analysis, which has been carried out to see the noise reduction in the tail of the PSDs, using the Welch method [4] with different averaging windows. The result was that, for small enough windows, the shape of the PSD at higher frequencies approached the best fit of the PSD. Therefore it was decided to use as input in the analyses the worst case and the best-fit cases for the PSDs of M1 and M2 as shown in Fig. 9 below. Being the worst case extremely penalized by the numeric noise in the treatment of the data, it is used only as reference.

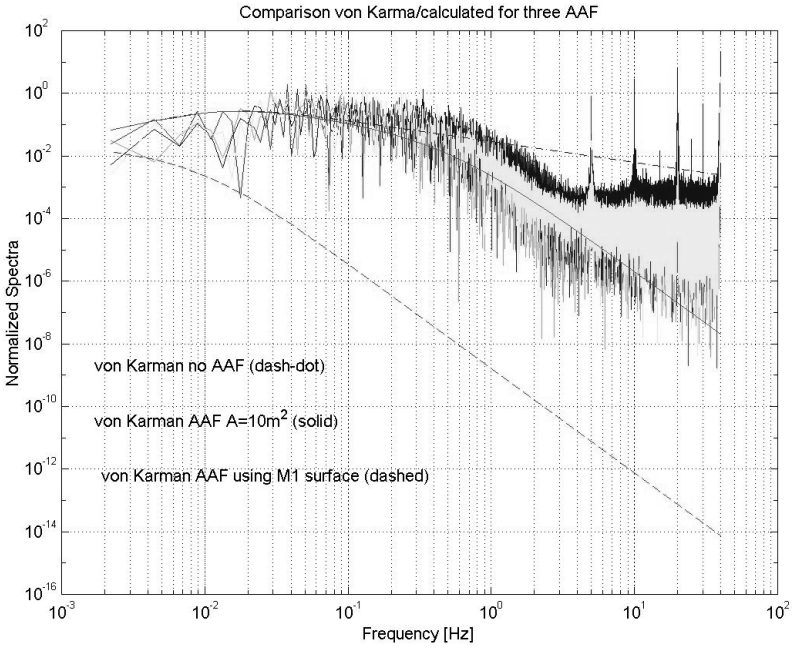

Figure 8: comparing von Karman spectrum corrected with three different aerodynamic admittance functions (AAF) with calculated PSDs.

Using a conservative approach the wind pressure is considered fully correlated both spatially and temporally on the individual optical surface, maximizing the deformations. On the contrary the PSD on different surfaces are considered fully uncorrelated, a valid assumptions in view of the separation between these two surfaces (~95 m).

The global reaction torque around the axes has been also calculated. The values resulted to be much smaller, about one tenth, of that used to dimension the drive system, namely about 0.5 MNm. This is a sign of the great importance of the statistical averaging of the forces on the telescope and a sign of statistical uncorrelation between PSDs.

It was said before that an uncritical use of usual wind loading theory would bring erroneous estimates of PSDs, with the possibility of dramatically underestimating energy content at higher. This is shown comparing the von Karman spectrum with the envelope spectrum calculated with PowerFLOW (Fig. 8).

Using the formulae as proposed would have underestimated the energy content at higher frequencies by a factor 10^6, while not using the aerodynamic admittance function would have overestimated in the mid range by a factor 100.

From this it becomes clear that in case of large structures an assessment of the wind PSD needs to be done using one of the last three methods described at the beginning.

4. RANDOM VIBRATION ANALYSIS

In order to evaluate the dynamic impact of the wind load on the structural performance of OWL, a random vibration analyses has been carried out with the FE Model of OWL by applying the pressure distribution obtained with the CFD analysis. The analysis procedure is based on computing statistics of each modal response and then combining them. Using the theory of random vibrations, the response PSD's can be calculated from the input PSD Sf(ω) with the help of transfer functions H(ω) and by using mode superposition techniques. The response PSD's are then given by

$$S_r(\omega) = S_f(\omega) * \left| H(\omega) \right|^2$$

With this response PSD one can derive statistical output data like mean square response and 1σ values. A more detailed description of the analysis can be found in [5].

The configuration of the FE Model corresponds to the one of the CFD analysis, i.e. altitude structure pointing 20° from zenith. A more detailed description of the FE model is presented in [6]. In order to obtain the modal response, a modal analysis has been performed to calculate the lowest 400 modes. The appropriate frequency range lies between 1.9 and 16.2 Hz. After the modal analysis a random vibration analysis was carried out by combining the modes and applying the pressure PSD.

The analyses are mainly based on conservative assumptions:

- Two different input PSDs were supplied in pressure versus frequency format, whereas one is uniformly applied on M1 and the other one on M2.
- Within each of the main mirrors, all the control points are fully correlated, whereas the M1 input PSD is fully uncorrelated from the M2 input PSD.
- The evaluation of the results is based on the maximum deflected node of each mirror surface.

In the framework of this report the results of the following three load cases will be presented:

1. Best-fit input PSD with building
2. Best-fit input PSD without building
3. Envelope (worst) input PSD with building (over-conservative)

In the first two load cases a sort of best-fit PSD has been applied, whereas in the 3rd one we used the envelope (worse) PSD. As already described in chapter 3, the best-fit PSD corresponds to a sort-of average curve over all the mirror control points PSDs. The "envelope" PSD has been produced by enveloping all the mirror control points PSDs including noise. Therefore, this load case is considered to be over-conservative and has been investigated for comparison reasons only. All the input PSD's are shown in Fig. 9 for M1 and M2, respectively.

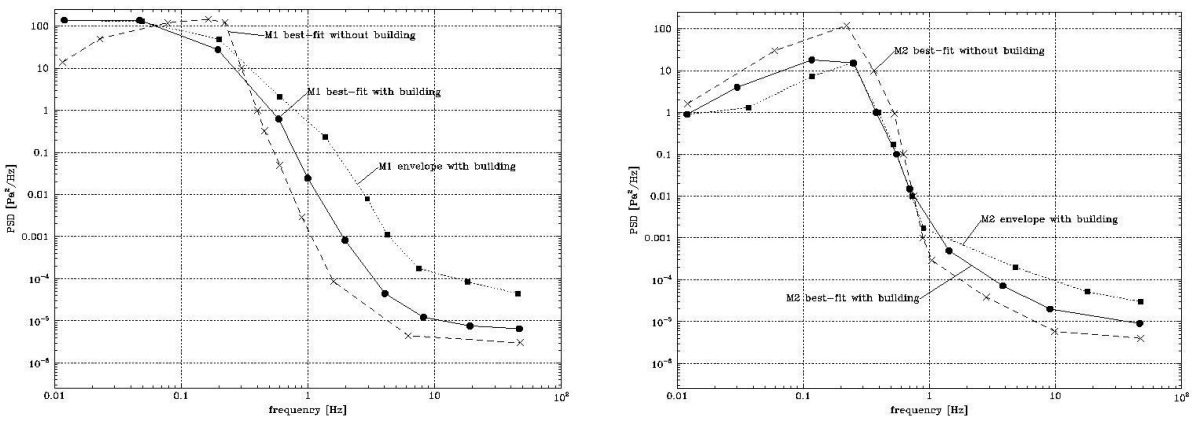

Figure 9: M1 (left) and M2 (right) input PSD's for all load cases.

The surface deformation over the whole frequency range has been evaluated in terms of the statistical 1σ probability of 68.3 %[1]. The contour plots in Fig. 10 represent the 1σ surface deflection of M1 and M2 for load case 1. The deformation shapes are dominated by the mode shape of the main piston mode of the structure at 3.7 Hz (see [6]). This deformation is superimposed to a tilt around the altitude axis, which is caused by the excitation of the locked rotor mode.

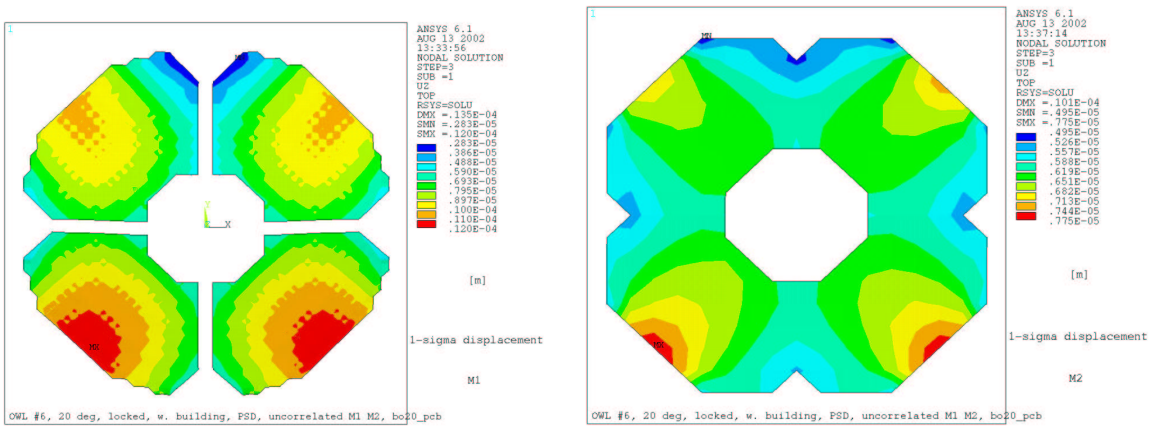

Figure 10: 1σ deflection of M1 (left) and M2 (right) for load case 1.

These effects are also visible in the response PSDs of individual nodes, because the highest peaks of the curves occur at 3.7 Hz and 2.1 Hz. In Fig. 11 shows the frequency dependent behavior of the maximum and minimum deflected nodes on the primary mirror for load case 1. The response curves feature the upper and lower boundaries of all the primary mirror nodes, i.e. all the other nodes are situated in between the two extreme curves. As indicated in Fig. 11, the 1σ (RMS) displacement of the maximum deflected node results in 13 µm for the frequencies below 1 Hz, 400 nm for frequencies between 1 and 5 Hz, and 80 nm for frequencies above 5 Hz. Due to its high wind energy content the highest contribution are in the low frequency range (< 1 Hz). However, these errors are considered to be controllable quasi-statically. The errors above 1 Hz are already within the range of adaptive optics.

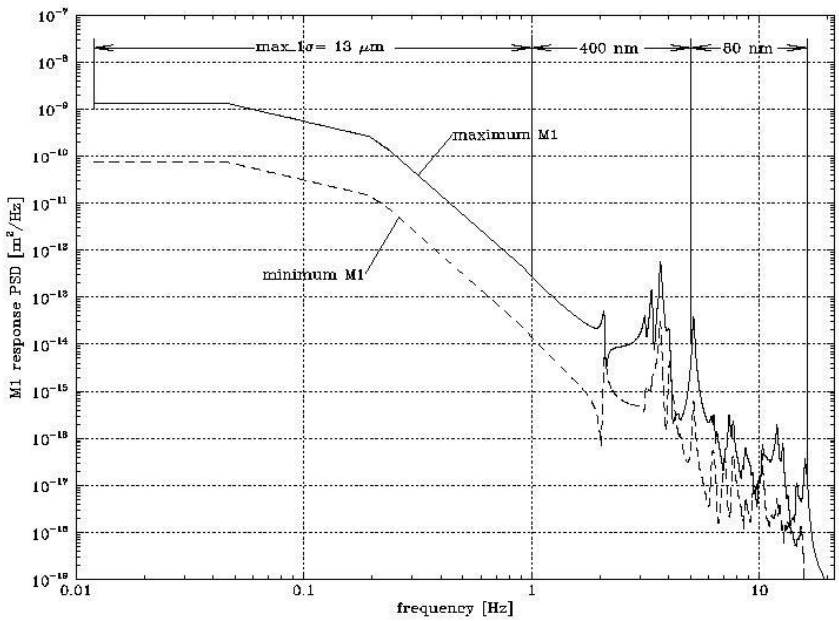

Figure 11: 1σ displacement of min. and max. M1 nodes for load case **1**

[1] The 1σ value can be interpreted as root mean square (RMS) value, and the 3σ as peak-to-valley (PTV).

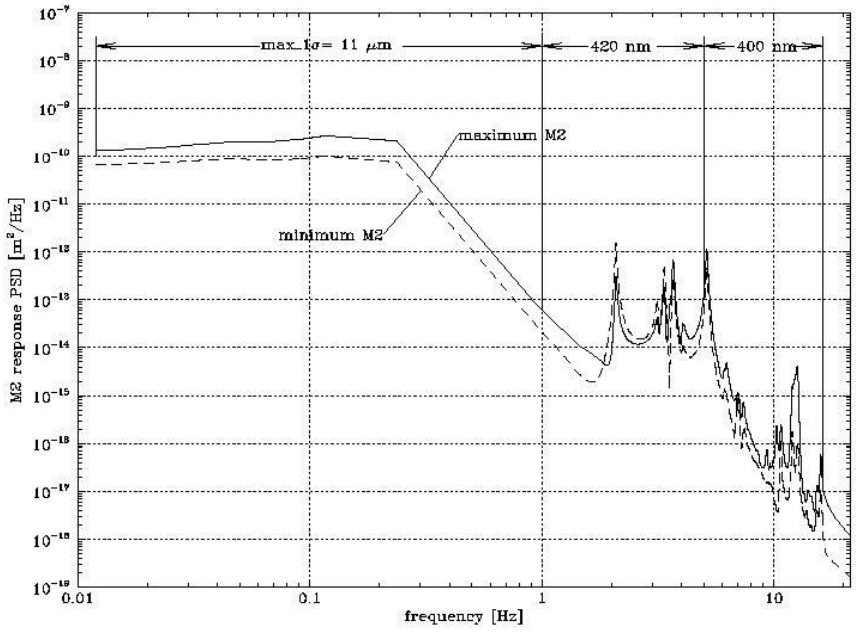

Figure 12: 1σ displacement of min. and max. M2 nodes for load case 1.

Fig. 12 represents the appropriate response curves and evaluation of the secondary mirror. It is remarkable, that the 1σ deflection of M2, compared to M1, is slightly smaller in the quasi-static range (11 μm) and about 5 times higher in the high frequency range (400 nm). This effect can be explained by the fact that the support structure of the secondary mirror is by nature less stiff and more sensitive to wind perturbations than the one of the primary. The highest response peaks of the secondary occurs at 2.1 Hz, which is the locked rotor frequency mode. This means, that beneath the piston mode at 3.7 Hz also the locked rotor mode shape has an important impact on the dynamic response of M2.

A comparison of all the load case results in terms of 1σ surface deflection is summarized in Tab. 1 for M1 and in Tab. 2 for M2. By comparing the first two load cases it is remarkable, that the 1σ response for higher frequencies (above 1 Hz) is by a factor 2 to 3 smaller without the maintenance building. In this case the surface deflection of M1 results in 148 nm between 1 and 5 Hz, and 42 nm above 5 Hz. The appropriate values for M2 are 189 nm and 219 nm, respectively. Compared to the 1st load case the 3rd load case, which is considered to be over-conservative, gives by a factor 3 to 8 larger values for the high frequency range.

Load case		1σ maximum displacement of M1 in [μm]			
Frequency range [Hz]:		0.012 to 1	1 to 5	5 to 16	Full range
1	Best-fit, with building	13.339	0.404	0.077	13.345
2	Best-fit, without building	20.770	**0.148**	**0.042**	20.771
3	Envelope, with building	16.032	2.490	0.259	16.226

Table 1: Comparison of 1σ maximum displacement of M1.

Load case		1σ maximum displacement of M2 in [μm]			
Frequency range [Hz]:		0.012 to 1	1 to 5	5 to 16	Full range
1	Best-fit, with building	10.966	0.419	0.404	10.982
2	Best-fit, without building	23.390	0.189	0.219	23.392
3	Envelope, with building	9.616	3.482	1.322	10.312

Table 2: Comparison of 1σ maximum displacement of M2.

5. CONCLUSIONS

Assessing wind PSDs is fundamental in the case of telescopes. In designing a telescope not only the absolute value of the deformation but also its frequency distribution is crucial to define a strategy in the design of the optomechanics and of the controls [7].
The first step taken at ESO has given a good insight in the effect of wind OWL, in particular on its main optical surfaces.
It has been shown that in the case of such large structure the assessment of the wind loading has to go through an *ad hoc* calculation or wind tunnel test, to avoid a misuse of the general established theory.
From the results it appears that the presence of a building in front of the telescope, although it decreases slightly the wind pressure at low frequencies, causes high frequency components to be larger. The results summarized in Table 1 seem to confirm the results of previous studies and the literature on the subject of turbulence induced by obstacles. This would suggest, as in theory expected, that to keep lower the magnitude of the deflection at higher frequencies it is better to operate the telescope in open wind. Trying to protect it with screens would decrease the quasi-static wind action component but would increase the energy content at higher frequencies, where the corrections would be more difficult to perform.
The deflections calculated in this study consider the PSDs correlated, which gives conservative results. In the next steps the same analyses will be repeated to take into account the actual uncorrelation, and one would expect deflections lower by about 20 to 30%.
The activities described in this paper are a first step in understanding the effect of wind on OWL.
The next steps will be to continue studying OWL in different positions to detect possible worse cases for wind loading. Activities are then foreseen in wind tunnel and also in using one of the existing 100m class radio telescopes to perform measurements on site, in order to cross check the results obtained with CFD.
It is not excluded to study also a protection of the telescope, and to verify its effect on the PSD.

REFERENCES

[1] T. Balendra: Vibration of buildings to wind and earthquake loads. Springer-Verlag 1993.

[2] Vickery B. J.: On the flow behind a coarse grid and its use as a model of atmospheric turbulence in studies related to wind loads in building. Nat. Phys. Lab. Aero. Report 1143, 1965.

[3] PowerFLOW® explanatory notes. http://www.exa.com/newsite/frames/powerflowmaster.html

[4] Welch, P. D.: The use of Fast Fourier Transform for the estimation of Power Spectra: a method based on time averaging over short modified periodograms. IEEE Trans. Audio Electroacoust. Vol. AU-15, June 1967.

[5] ANSYS Release 6.1, Theory Reference Manual, ANSYS Inc., Canonsburg

[6] E. Brunetto, F. Koch, F. Biancat Marchet, M. Dimmler, Friction drive and bogies for OWL's main axes, technological step backwards or cost effective alternative? SPIE 2002 Kona

[7] Ph. Dierickx et al.: Eye of the beholder: designing OWL, SPIE 2002 Kona.